arXiv:1601.04672v1 [cs.ET] 18 Jan 2016

Physical maze solvers. All twelve prototypes implement 1961 Lee algorithm.

Andrew Adamatzky

Abstract We overview experimental laboratory prototypes of maze solvers. We speculate that all maze solvers implement Lee algorithm by first developing a gradient of values showing a distance from any site of the maze to the destination site and then tracing a path from a given source site to the destination site. All prototypes approximate a set of many-source-one-destination paths using resistance, chemical and temporal gradients. They trace a path from a given source site to the destination site using electrical current, fluidic, growth of slime mould, Marangoni flow, crawling of epithelial cells, excitation waves in chemical medium, propagating crystallisation patterns. Some of the prototypes visualise the path using a stream of dye, thermal camera or glow discharge; others require a computer to extract the path from time lapse images of the tracing. We discuss the prototypes in terms of speed, costs and durability of the path visualisation.

Andrew Adamatzky
University of the West of England, Bristol, UK e-mail: andrew.adamatzky@uwe.ac.uk

Contents

Physical maze solvers. All twelve prototypes implement 1961 Lee algorithm. 1
Andrew Adamatzky
1 Introduction 3
2 Resistance gradient 5
2.1 Electrical current 5
2.2 FLUIDIC: Fluidic 7
2.3 PHYSARUM I: Slime mould 7
3 Diffusion gradient 7
3.1 MARANGONI: Marangoni flow 8
3.2 Living cells 8
4 Temperature gradient: TEMPERATURE 9
5 Temporal gradient 10
5.1 VLSI: VLSI array processor 10
5.2 WAVE: Excitation waves 10
5.3 CRYSTALL: Crystallization 11
6 Analysis 11
7 Discussion 12
References 14

1 Introduction

To solve a maze is to find a route from the source site to the destination site. If there is just a single path to the destination the maze is called a labyrinth. To solve a labyrinth one must just avoid dead ends. In a maze there are at least two paths leading from the entrance to the exit. To solve a maze one must find a shortest path. Not rarely concepts of 'maze', 'labyrinth' and 'collision-free shortest path' are mixed in experimental laboratory papers. We will not differentiate either. All algorithms and physical prototypes that solve shortest collision-free path on a planar graph solve mazes [14]. All algorithms and prototypes that solve mazes solve labyrinths.

There are two scenarios of the maze problem: the solver does not know the whole structure of the maze and the solver knows the structure of the maze.

The first scenario — we are inside the maze – is the original one. This is how Theseus, the Shannon's maze solving mechanical mouse, was born [48].[1] The mouse *per se* was a magnet with copper whiskers. The mechanism was hidden under the maze. A circuit with hundred of relays and mechanical drives grabbed the mouse from below the floor and moved to a randomly chosen direction. When the mouse detected an obstacle with its whiskers the underfloor mechanism moved the mouse away from the obstacle and other direction of movement has been selected. The task was complemented when the destination site was found. Being placed at any site of the maze the mouse was able to find a path towards the destination site. Several electro-mechanical devices have been built in 1950-1970, including well know Wallace's maze solving computer [57]. The Theseus also inspired a range of robotic mice competitions [61]. The algorithms of a maze traversing agent, see overviews in [58, 12] include random walk [10]; the Dead Reckoning (the mouse travels straight, when it encounters a junction it turns randomly, when it finds itself in the dead end it turns around), Dead End Learning (the agent remembers dead ends and places a virtual wall in the corridor leading to each dead end); Flood Fill (the agent assigns a distance, as crow flies, to each site of the maze and then travel in the maze and updates the distance values with realistic numbers); and, Pledge algorithm where the maze traversing agent is equipped with a compass, which allows to maintain a predetermined direction of motion (e.g. always north); the intersections between the corridors oriented north-south and walls are treated as graph vertices [14, 1]. Hybrids of the Wall Follow and the Pledge algorithms are used in industrial robotics and space explorations: a robot knows coordinates of the destination site, has a compass, turns on a fixed angle and counts turns [33, 32].There are also genetic programming and artificial neural networks for maze solving [26].

The second scenario of maze solving — we are above the maze — is the one we study here. In 1961 Lee proposed the algorithm [30, 46] which became one of the most famous, reused and rediscovered algorithms in last century. We start at the destination site. We label neighbours of the site with '1'. Then we label their neighbours with '2'. Being at the site labelled i we label its non-yet-labelled neighbours with $i + 1$. Sites occupied by obstacles, or the maze walls, are not labelled. When all accessible sites are labelled the exploration task is completed. To extract the path from any given site of the maze to the destination site we start at the source site. Then we select a neighbour of the source site with lowest value of its label. We add this neighbour to the list. We jump at this neighbour. Then we select its neighbour with lowest value of the label. We add this neighbour to the list. We jump at this neighbour. We continue like that till we get at the destination site. Thus the algorithm computes one-destination-many-sources shortest path. A set of shortest path starting from each site of the maze gives us a spanning tree which nodes are sites of the maze and a root is the site where wave pattern of labelling started to grow. In robotics the Lee algorithm was transformed into a potential method pioneered in [38] and further developed in [59, 24]. The destination is assigned an infinite potential. Gradient is calculated locally. Streamlines from the source site to the destination site are calculated locally at each site by selecting locally maximum gradient [16]. Also, some algorithms assume that the destination has an 'attracting' potential and obstacles are 'repellents' [27, 6, 8].

Most experimental laboratory prototype of maze solvers implement the Lee algorithm. The gradients developed are resistance (Sect. 2), chemical (Sect. 2), temporal (Sect. 2) and thermal (Sect. 2). The paths are traced along the gradients by electrical current (Sect. 2.1), fluids (Sect. 2.2), cellular cytoplasm (Sect. 2.3), Marangoni flow (Sect. 3.1), living cells (Sect. 3.2), excitation waves

[1] See `http://cyberneticzoo.com/mazesolvers/`

(Sect. 5.2) and crystallisation (Sect. 5.3). We present brief descriptions of known experimental laboratory prototypes of maze solvers and analyse them comparatively.

2 Resistance gradient

Imagine a maze filled with hard balls. The entrance and the exist are open. We put our hand in the entrance and push the balls. Balls in the dead ends have nowhere to move. The pressure is eventually transferred to the balls nearby exit. These balls start falling out. We add more balls thought entrance and push again. Balls fall out through the exit. Thus a movement of balls is established. The balls are moving along the shortest path between the entrance and the exit. The balls explore the maze in parallel and 'calculate' the path from the exit to the entrance. In this section we discuss prototypes which employe electrical and hydrodynamic resistances.

2.1 Electrical current

Approximation of a collision-free path with a network of resistors is proposed in [52, 53]. A space is discretised as a resistor network. The resistors representing obstacles are insulators or current thinks. Other resistors have the same initial resistance. An electoral power source is connected to the destination and the source sites. The destination site is the electrical current source [15]. Current flows in the grid. Current does not flow into obstacles. To trace the path one must follow a current streamline by performing gradient descent in electrical potential. That is for each node a next move is selected by measuring the voltage difference between current node and each of its neighbours, and moving to the neighbours which shows maximum voltage. We are not aware of any large-scale prototype of such path solver. Two VLSI processors have been manufactured [49]. They feature 16×16 and 18×18 cells, 2 μm nwell SCMOS technology, 3960 μ × 4240'μ and 4560 μ×4560 μ frame size, 16-bit asynchronous data bus. For gradient descent the source is 5 V and the destination is 0 V, and *vice verse* for gradient ascent.

There are two ways to represent walls of a maze [15]: Dirichlet boundary conditions and Neumann boundary conditions. When the Dirichlet boundary conditions is adopted the walls, or obstacles, have zero electrical potential and act as sinks of the electrical current [16]. Then the current lines are perpendicular to the walls and an agent, e.g. a robot, travelling along the current lines stays away from the walls [15]. In case of the Neumann boundary conditions the walls are insulators [52]. The walls are not 'felt' by the electrical current. Then the current lines are parallel to the walls. This gives the travelling agent less clearance. The original approach of [52] has been extended to networks of memristors (resistors with memory) [39], which could allow for computation of a path in directed planar graph.

A shortest path can be visualised, though not digitally recorded, without discretisation of the space. A maze is filled with a continuous conductive material. Corridors are conductors, walls are insulators. An electrical potential difference is applied between the source and the destination sites. The electrical current 'explores' all possible pathways in the maze. As proposed in [11] the electrons, driven by the applied electrical field, move along the conductive corridors in a maze until they encounter dead end or the destination site. When the electrons reach dead end they are

cancelled inside the conductor. The electric field inside the dead ends becomes zero. The flow of electrons on the conductive pathways leading the destination does not stop. Thus the electrical flow calculates the shortest path. This path is detected via glow-discharge or thermo-visualisation.

2.1.1 GLOW: Glow-discharge visualisation

This maze solver is proposed in [43]. A drawing of a maze is transferred on a glass wafer and channels are etched in the glass. The channels are c. 250 μm wide and c. 100 μm deep. Electrodes are inserted in the source and the destination sites. The glass maze is covered tightly and filled with helium at 500 Torr. A voltage of up to 30 kV, above the breakdown voltage, is applied. Luminescence of the discharge shows the shortest path in the maze. Shortest path is visualised in 500 ms.

A maze solver using much less pressure and much lower voltage is proposed in [17]. The maze is made of a plexiglas disk, diameter 287 mm, 50 mm height. Channels 25 mm wide and 40 mm deep are cut in the disk. Hole for the anode is made in the center of the disk. Cathode is placed in the destination site. The maze is filled with air, pressure 0.110 Torr. A gas-discharge chamber is made of polyamide in 450 mm diameter and 50 mm height, copper cathode in the form of rectangular plate of 158 mm^2 size is fitted on its side surface in a cathode holder. The maze is placed in the gas-discharge chamber. Stainless steel rod anode of 10 mm diameter is placed at the center of the chamber. Voltage of 2kV is applied between the electrodes. The path is visualised by the glow of ionised air in the maze's channels. Experiments [17] also demonstrate propagation of striations, the ionisation waves [28], along the path.

2.1.2 ASSEMBLY: Assembly of nano particles

The maze is solved with nano particles in [34]. A maze is made of polydimethylsilicoxane and filled with silicon oil. A drop of a dispersion of conductive nano particles: spherical copper nano particles 10 μm diameter and metallic carbon nanotubes 10 μm long — is added at the source site. An electrical potential 1–5 kV is applied between the source and the destination. The particles diffusing from the source site become polarised. The polarised particles experience dipole interactions. The dipole interactions make the particles to form a chain along line of the electric field with maximal strength. The chain is formed to maximise the electrical current and to minimise the potential drop. The chain of the particles forms a conductive bridge between the electrodes at the source site and the destination site which represents the shortest path.

2.1.3 THERMO: Thermo-visualisation

A maze solver using electrical current is proposed in [11]. The prototype employs thermal visualisation of the electrical current. A maze 10×10 cm is made from copper tracks on a printed board. Copper tracks represent corridors. The electrical current 2.4 A is applied between the source and the destination sites. The flow of electrons heats the conductor, due to Joule heating. A local temperature of the conductor is proportional to intensity of the flow. In experiments [11] the temperature along the shortest path increased by c. 10^{o}C. The heating is visualised with the infrared camera. The shortest path is represented by the brightest loci on the thermographic image.

2.2 FLUIDIC*: Fluidic*

In a fluidic maze solver developed in [18] a maze is the network of micro-channels. The network is sealed. Only the source site (inlet) and the destination site (outlet) are open. The maze is filled with a high-viscosity fluid. A low-viscosity coloured fluid is pumped under pressure into the maze, via the inlet. Due to a pressure drop between the inlet and the outlet liquids start leaving the maze via the outlet. A velocity of fluid in a channel is inversely proportional to the length of the channel. High-viscosity fluid in the channels leading to dead ends prevents the coloured low-viscosity fluid from entering the channels. There is no pressure drop between the inlet and any of the dead ends. Portions of the 'filler' liquid leave the maze. They are gradually displaced by the colour liquid. The colour liquid travels along maximum gradient of the pressure drop, which is along a shortest path from the inlet to outlet. When the colour liquid fills in the path the viscosity along the path decreases. This leads to increase of the liquid velocity along the path. The shortest path — least hydrodynamic resistance path — from the inlet to the outlet is represented by channels filled with coloured fluid.

In the experiments [18] channel width varied from c. 90 μm to 200 μm, maze size c. 40×50 mm. The maze is filed with ethanol-based solution of bromophenoll. A dark coloured solution of a food dye in mix of water and ethylene glycol is injected in the maze at a constant flow, velocity c 5–10 mm/sec. A drop of pressure between the inlet and the outlet is c. 0.75-2.25 Torr. The channels along the shortest path become coloured. The path is visualised in half-a-minute.

2.3 PHYSARUM I*: Slime mould*

The prototype based on reconfiguration of protoplasmic network of acellular slime mould *Physarum polycephalum* is proposed in [35]. The slime mould is inoculated everywhere in a maze. The slime mould develops a network of protoplasmic tubes spanning all channels of the maze. Oat flakes are placed in the source and the destination site. A tube lying along the shortest (or near shortest) path between sites with nutrients develop increased flow of cytoplasm. This tube becomes thicker. Tubes branching to sites without nutrients become smaller due to lack of cytoplasm flow. They eventually collapse. The sickest tube represents the path between the sources of nutrients, and therefore, the path between the source and the destination sites. The selection of the shortest protoplasmic tube is implemented via interaction of propagating bio-chemical, electric potential and contractile waves in the plasmodium's body, see mathematical model in [54].

3 Diffusion gradient

A source of a diffusing substance is placed at the destination site. After the substance propagates all over the maze a concentration of the substance develops. The concentration gradient is steepest towards the source of the diffusion. Thus starting at any site of the maze and following the steepest gradient one can reach the source of the diffusion. The diffusing substance represents one-destination-many-sources shortest paths. To trace a shortest path from any site, we place a chemotactic agent at the site and record its movement towards the destination site.

3.1 MARANGONI*: Marangoni flow*

A diffusion gradient determines a surface tension gradient. A flow of liquid runs from the place of low surface tension to the place of high surface tension. This flow transports droplets. A maze solver proposed in [29] is as follows. A maze is made of polydimethylsiloxane, size c. 16 × 16 mm, channels have width 1.4 mm, and walls are 1 mm high. The maze is filled with a solution of potassium hydroxide. A surfactant is added to reduce the liquid's surface tension. An agarose block soaked in a hydrochloric acid is placed at the destination site. In c. 40 s a pH gradient establishes in the maze. Then a 1 μL droplet of a mineral oil or dichloromethane mixed with 2-hexyldecanoic acid is placed at the source site. The droplet does not mix with the liquid filling the maze. The droplet moves along the steepest gradient of the potassium hydroxide. The steepest gradient is along a shortest path. Exact mechanics of the droplet's motion is explained in [29] as follows. Potassium hydroxide, which fills the maze, is a deprotonating agent. Molecule of the potassium hydroxide removes protons from molecules of 2-hexyldecanoic acid diffusing from the droplet. A degree of protonation is proportional to concentration of hydrochloric acid, diffusing form the destination site. Protonated 2-hexyldecanoic acid at the liquid surface determines the surface tension. The gradient of the protonated acid determines a gradient of the surface tension. The surface tension decreases towards the destination site. A flow of liquid — the Marangoni flow — is established from the site of low surface tension to the site of high surface tension, i.e. from the start to the destination site. The droplet is moved by the flow [29]; see also discussion on mobility of surface in [40] and more details on pH dependent motion of self-propelled droplets in [13].

In the prototype [29] a path from the start site to the destination site is traced by a droplet but not visualised. To visualise the path fully one must record a trajectory of the droplet. A visualisation is implemented in [31]. A dye powder, Phenol Rd, is placed at the start site. The Marangoni flow transports the dye form the start to the destination. The coloured channels represent a path connecting the source site and the destination.

Another prototype of a droplet maze solver is demonstrated in [56]. The maze c. 45×75 mm in size, with channels c. 10 mm wide, is filled with water solution of a sodium decanoate. A nitrobenzene droplet loaded with sodium chloride grains is placed at the destination site. A 5 muL decanol droplet is placed at the source site. The sodium chloride diffuses from its host nitrobenzene droplet at the destination site. A gradient of salt is established. The gradient is steepest along a shortest path leading from any site of the maze to the destination site. A decanol droplet moves along the steepest gradient till the droplet reaches the nitrobenzene with salt droplet at the destination site.

3.2 Living cells

A source of a chemo-attractant is placed at the destination site. The chemo-attractant diffuses along the channels of the maze. It reaches the destination site eventually. The maximum gradient is along the shortest path from any given site of a maze to the destination site. A living cell is placed at the source site. The cell follows the maximum gradients thus moving along the shortest path towards the destination site.

3.2.1 PHYSARUM II: Slime mould

The slime mould maze solver based on chemo-attraction is proposed in [4]. An oat flake is placed in the destination site. The slime mould *Physarum polycephalum* is inoculated in the source site. The oat flakes, or rather bacterias colonising the flake, release a chemoattractant. The chemo-attractant diffuses along the channels. The Physarum explores its vicinity by branching protoplasmic tubes into openings of nearby channels. When a wave-front of diffusing attractants reaches Physarum, the Physarum halts the lateral exploration. Instead it develops an active growing zone propagating along the gradient of the attractant's diffusion. The problem is solved when Physarum reaches the source site. The sickest tube represents the shortest path between the destination site and the source site. Not only nutrients can be placed at the destination site but any volatile substances that attract the slime mould, e.g. roots of the medicinal plant *Valeriana officinalis* [45].

3.2.2 EPITHELIUM: Epithelial cells

Experimental maze solver with epithelial cells is proposed in [47]. Epithelial cells move towards sites with highest concentration of the epidermal growth factor (EGF). An epithelial cell uptakes EGF. Thus the cell depletes EGF's concentration in the cell's vicinity. A 400 μm$\times$400 μm maze is made of orthogonal channels c. 10 μm wide [47]. The channels are filled with epithelium culture medium. There is a uniform distribution of the EGF inside the maze at the beginning of an experiment. The maze is placed in the medium with 'unlimited' supply of EGF. A cell is placed at the entrance channel. The cell enters the maze and crawls along its first channel. The cell consumes EGF and decreases EGF concentration in its own neighbourhood. EGF from all channels, accessible from the current position of the cell, diffuses towards the site with low concentration. Supply of EFG in channels ending with dead ends is limited. Unlimited supply of EGF into the maze is provided via exit channel. An EGF diffusion gradient from the exit through the maze to dead ends and the entrance is established. The cell follows the diffusion gradient. The gradient is maximum along the shortest path. The cell moves along the shortest path towards the exit.

4 Temperature gradient: TEMPERATURE

A Marangoni flow is a mass-transfer of a liquid from a region with low surface tension to a region with high surface tension [31]. The mass transfer can move droplets, or any other objects, or dyes. Any methods of establishing a surface tension gradient is OK for tracing a shortest path with Marangoni flow. In [31] a temperature gradient is used. A maze is made from polydimethylsiloxane with channels 1.4 mm wide and 1 mm deep. The maze is filled with hot, c. 99°C, aqueous solution of sodium hydroxide with hexyldecanoic acid. A steel sphere, diameter 4 mm, is cooled with dry ice and placed at the destination site in the maze. A phenol red dye powder is placed on the surface of the liquid at the start site. The cold sphere creates temperature gradient. The temperature gradient creates a surface tension gradient. The Marangoni flow is established along a shortest path from any site of the maze to the destination site. The dye powder applied at the source site is dragged by the flow towards the destination site. The trace of the dye represents the shortest path.

5 Temporal gradient

A wave front advances for a fixed distance per unit of time in a direction normal to the front. A wave generated at the source site of a maze reaches the destination site along the shortest path. The wave 'finds' the exit. We just need to record the path of the wave.

5.1 VLSI*: VLSI array processor*

An array processor solving shortest path over terrain with elevations is reported in [25]. This is a digital processor of 24 × 25 cells, manufactured with 2 μm CMOS. A cell size is 296 μm × 330 μm, the processor's size is 7.9 mm × 9.2 mm. An elevations map is encoded to 255 levels of grey and loaded into the processor array. A signal is originated at the destination site. Wave-front of the signal propagates on the array. Each cell delays a signal by time proportional to the 'elevation' value loaded into the cells. Then the cell broadcasts the value to its neighbours. When a processor receives signal, the incoming signal direction is stored and further inputs to the cell are ignored. Starting from each cell we can follow the fastest path towards the destination site.

5.2 WAVE*: Excitation waves*

In [50] a labyrinth solution in excitable chemical medium is proposed. A c. 3×3 cm labyrinth is made of vinyl-acrylic membrane. The membrane is saturated with Belousov-Zhabotinsky (BZ) mixture. Impenetrable walls are made by cutting away parts of the membrane. The channels are excitable. The walls are non-excitable. Excitation waves are initiated at the source site by touching the membrane with a silver wire. The wave-fronts propagate with a speed of c. 2 mm/min. Dynamics of the waves is recorded with 50 sec intervals. The locations of the wave-fronts are colour-mapped: the colour depends on the time of recording. A shortest path from the source site to the destination site is extracted from the time lapse colour maps. In this setup excitation waves explore the labyrinth but the path is extracted by a computer.

The approach is slightly improved in [9]. By recording time lapse images of excitation wave fronts propagating in a two-dimensional medium we can construct a set of isochrones: lines which points are at the same distance from the site of the wave origination. By extracting intersection sites of isochrones of waves propagating from the source site to the destination site with isochrones of waves propagating from the destination site to the source site we can extract the shortest path. Experiments report in [9] deal not with a maze but a space with two obstacles. The approach would work in the maze as well. The BZ medium does not do any computation. The results are obtained on a computer by analysing dynamics of the excitation wave fronts. Something is better than nothing: the approach is successfully used in unconventional robotics [7, 6].

Another BZ based maze solver is proposed in [42]: it exploits light-sensitive BZ reaction. Extraction of the path requires an extensive image analysis of the excitation dynamics, therefore this prototype is not worthy of discussion here.

5.3 CRYSTALL*: Crystallization*

In [2] we proposed that a propagating excitation wave-front sets up pointers at each site of the medium. The pointers indicate a direction from where the wave-fronts came from. A shortest path towards the the source of the excitation can be recovered by following the pointers. This approach is experimentally implemented in [3] where crystals play a role of pointers. A set of one-source-many-destinations shortest path in a room with obstacles is constructed using crystallisation of sodium acetate trihydrate [3]. The room with obstacles is technically a maze with irregularly shaped walls. Obstacles are made of an adhesive resin attached to a bottom of a Petri dish. A super-saturated clear solution of sodium acetate trihydrate is poured into the Petri dish. The solution is cooled down. A crystallisation is induced by briefly immersing an aluminium wire powdered with fine crystals of the sodium acetate into the target site in the solution. Crystals growing from nucleation sites bear distinctive elongated shapes expanding towards their proximal ends. Not only a crystal's overall shape but also the orientation of saw-tooth edges indicate the direction of the crystal's growth. The crystallisation patterns compete for space. A crystallisation pattern following longer than shortest path is unable to reach the source site because the space available is already occupied by the crystallisation pattern following the shortest path. Thus the direction of crystal growth can be detected by conventional image processing techniques, e.g. edge detection procedures, or by a complementary method of detecting directional uniformity of image domains. A configuration of local vectors, which indicate direction of crystallisation propagation, is calculated. A vector at each point indicates the direction from where the wave of crystallisation came from.

6 Analysis

With regards to time it takes the prototypes to solve the maze, i.e. to produce a traced path from the source to the destination, we can split the solvers into three groups:

- solve instantly (milliseconds or less): GLOW, THERMO, VLSI, CRYSTALL
- solve in minutes: ASSEMBLY, FLUIDIC, MARANGONI, TEMPERATURE, WAVE
- solve in hours: PHYSARUM I, PHYSARUM II, EPITHELIUM

The classification is very rough. We estimate the solution times based on reported sizes of mazes and expected propagation time of substances or perturbations in the maze solving substrates.

Only CRYSTALL visualises a gradient. Other prototypes do not. In CRYSTALL maze solver the temporal gradient can be seen by an unaided eye as a pattern of crystal needles.

With regards to path tracing two groups can be specified:

- path is visible as a state of the solver, no computer is necessary: GLOW, THERMO, ASSEMBLY, FLUIDIC, MARANGONI, TEMPERATURE, PHYSARUM I, PHYSARUM II,
- a computer is necessary to extract the path from the states of the solver: VLSI, CRYSTALL, WAVE, EPITHELIUM

In MARANGONI no computer assistance is required if the path is traced using dyes. If the path is traced by a mobile droplet then we must record time lapse images of the travelling droplet and extract the path form the images. In EPITHELIUM, if a single cells is used to trace the path then time lapse recording is necessary. However, if we send a procession of epithelial cells, following one

another, the path will become visible as a chain of cells. Because CRYSTALL and WAVE definitely require an external computing device to visualise the path we exclude them from further analyse. We also exclude VLSI because it a conventional hardware.

Several maze solvers are 'too demanding' in their requirements. Thus, GLOW requires up to 0.1–500 Torr pressure and 2–30 kV electrical potential; ASSEMBLY requires 1 kV electrical potential; FLUIDIC requires 0.7 – 2 Torr pressure, and TEMPERATURE requires fluid to be scalding hot.

Let us check five remaining prototypes: THERMO, MARANGONI, PHYSARUM I, PHYSARUM II, EPITHELIUM. The prototypes MARANGONI and EPITHELIUM are not ideal because they require some kind of a lab equipment not just a maze. The prototype PHYSARUM I is computationally inefficient because it requires the slime mould to be placed in all channels of the maze.

The remaining 'contestants' are THERMO and PHYSARUM II. Both prototypes are easy to make without a specialised lab equipment, and the whole setup of an experiment can be implemented in few minutes. It takes hours for PHYSARUM II to trace and to visualise the path. The prototype THERMO calculates the path instantly.

To conclude, the maze solver THERMO is the fastest and the easiest to implement physical maze solver. However, the THERMO does not visualise the path. We need a thermal camera to see the path. The PHYSARUM II visualises the path by morphology of the slime mould cell. However, the PHYSARUM II 'computes' the maze in many hours.

7 Discussion

The experimental laboratory prototypes of maze solvers might look differently but they all implement the same two tasks. First, they explore mazes in parallel and develop resistance, chemical, thermal or temporal gradients. Thus they approximate a one-destination-many-sources set of shortest paths. Second, they trace a path from a given source site to the destination site using fluid flows, electricity or living cells. Paths traced with electricity or flows are visualised with glow-charge gas, thermal camera, droplets, dyes. Paths traced with slime mould do not require any additional visualisation. Paths approximated with excitation wave-fronts or crystallisation patterns are visualised on computers.

A comparative plot of the maze solvers is shown in Fig. 1. We estimated speeds of maze solving from the experimental laboratory results reported, scaling all mazes to the same size. We estimated 'costs of prototyping' based on descriptions of experimental setups. The 'costs' are not in monetary terms but include fuzzy estimates of efforts necessary to prepare a maze, experimental setup, auxiliary equipment, and an inconvenience of using extreme physical parameters. For example, the glow-discharge maze solver requires a high pressure of gas filling the maze and very high electrical potential; the maze solver exploiting temperature gradients demands filling fluid to be scalding hot.

We have not discussed optical maze solving because we found reports only of theoretical designs [23, 37, 22]. In [23] the symmetrical properties of optical systems are utilised, the light diffraction is calculated and the path is extracted based on minimisation of the optical interferences. A detailed design of a two-dimensional nonlinear Fabry-Perot interferometer for maze solving is proposed in [37]. The optical solutions are interesting but impractical because they require a maze to be equipped with mirrors, so the light explores all paths in parallel; and, every junction of the maze channels must be checked with interferometer. Also, to trace the path one must analyse all data on a computer.

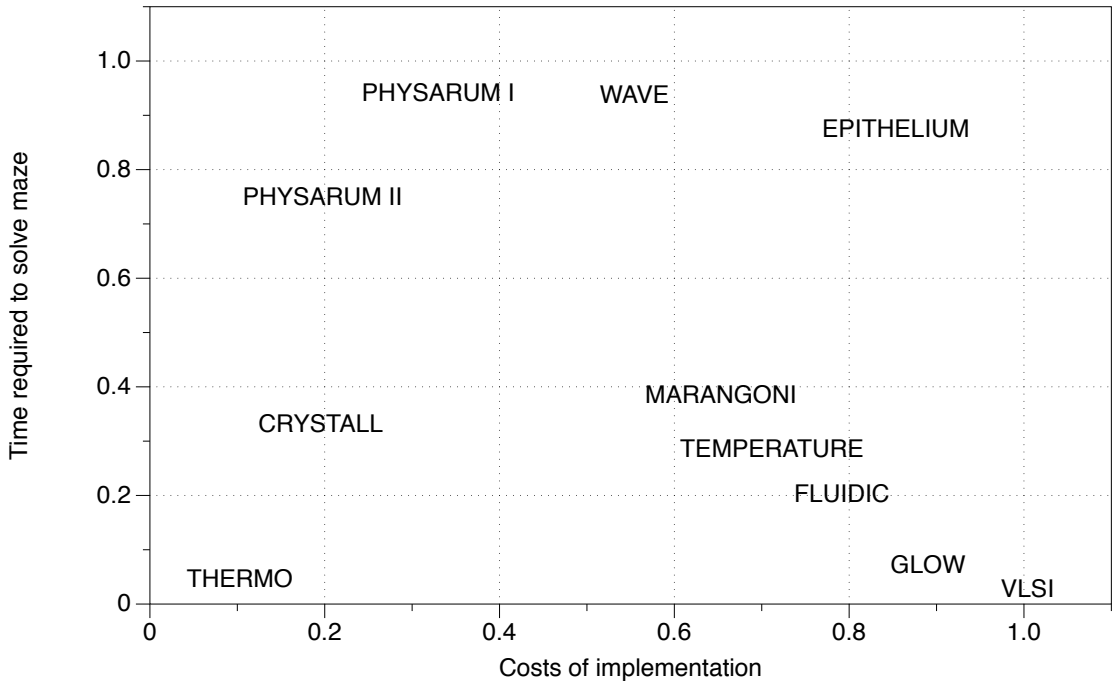

Fig. 1 Scatter plot of physical maze solvers based on estimated efforts of their prototyping and speed of maze solving.

We have not included any results on solving mazes with living creatures but the slime mould. Most papers published on experimental laboratory 'maze solving' by living creatures do actually mean animals learning to make a left turn or a right turn in 'T'- or'Y'-shaped junctions, as reported for ants [51], honey bees [62], nematodes [41]. Ants can approximate shortest paths [55, 19, 20, 36]. Chances are high the ants can solve complex (not just 'T'-junctions) mazes. Some of the laboratory results, e.g. chemotactic behaviour and learning of nematodes [44, 41], are enriched by simulations of a bit more complex than just 'Y'-junction mazes. Whatever case, most living creatures will not display the whole path in a maze. Slime mould does. In principle, plant roots can do as well.

With regards to plants, apexes of plant roots show chemotactic behaviour. The roots can make a choice between direction of motion in Y-shape junctions and select a route towards the attractant [60]. Experiments on plant root maze solving, where gravity is the only guiding force, were not successful because the roots often stuck in a dead end [5]. This is not surprising thought cause the gravity does not provide a length-dependent tracing of a path. More experiments should be done in future with plant roots.

Do humans employ gradient developing and subsequent path tracing techniques when they solve maze visually? Given a full structure of a maze, i.e. being above the maze, humans solve the maze by scanning the maze, memorising critical cues and then tracing the path visually [63]. The phases of the maze exploration and the path tracing are clearly distinct. These phases can be seen as roughly corresponding to the gradient developing phase and the path tracing, or visualisation, phase. There is a chance that a topological model of a maze is 'physically' mapped onto a neuronal activity of a

human brain cortex, where some neurons or their ensembles play a role of obstacles, other neurons are responsible for developing a gradient, and some neurons are responsible for tracing the path. In [21] a neuronal activity in superior parietal lobule of human subjects solving the maze is recorded with a whole-body magnetic resonance imaging and spectroscopy system. A mental traversing of the maze path is reflected in directional tuning of the volume unit. As [21] suggest, this might indicate an existence of a directionally selective synaptic activity of spatially close neuronal ensembles. Micro-volumes of the parental lobe showing absence of tuning might be corresponding to obstacles of the maze.

References

1. Harold Abelson and Andrea DiSessa. *Turtle geometry: The computer as a medium for exploring mathematics*. MIT press, 1986.
2. Andrew Adamatzky. Cellular automaton labyrinths and solution finding. *Computers & Graphics*, 21(4):519–522, 1997.
3. Andrew Adamatzky. Hot ice computer. *Physics Letters A*, 374(2):264–271, 2009.
4. Andrew Adamatzky. Slime mold solves maze in one pass, assisted by gradient of chemo-attractants. *NanoBioscience, IEEE Transactions on*, 11(2):131–134, 2012.
5. Andrew Adamatzky. Towards plant wires. *Biosystems*, 122:1–6, 2014.
6. Andrew Adamatzky and Benjamin de Lacy Costello. Collision-free path planning in the Belousov-Zhabotinsky medium assisted by a cellular automaton. *Naturwissenschaften*, 89(10):474–478, 2002.
7. Andrew Adamatzky, Benjamin de Lacy Costello, Chris Melhuish, and Norman Ratcliffe. Experimental implementation of mobile robot taxis with onboard Belousov–Zhabotinsky chemical medium. *Materials Science and Engineering: C*, 24(4):541–548, 2004.
8. Andrew Adamatzky and Christof Teuscher, editors. *From utopian to genuine unconventional computers*. Luniver Press, 2006.
9. K Agladze, N Magome, R Aliev, T Yamaguchi, and K Yoshikawa. Finding the optimal path with the aid of chemical wave. *Physica D: Nonlinear Phenomena*, 106(3):247–254, 1997.
10. Romas Aleliunas, Richard M Karp, Richard J Lipton, Laszlo Lovasz, and Charles Rackoff. Random walks, universal traversal sequences, and the complexity of maze problems. In *FOCS*, volume 79, pages 218–223, 1979.
11. Simon Ayrinhac. Electric current solves mazes. *Physics Education*, 49(4):443–446, 2014.
12. Michał Babula. Simulated maze solving algorithms through unknown mazes. *Organizing and Program Committee*, page 13, 2009.
13. Takahiko Ban, Tomoko Yamagami, Hiroki Nakata, and Yasunori Okano. pH-dependent motion of self-propelled droplets due to Marangoni effect at neutral pH. *Langmuir*, 29(8):2554–2561, 2013.
14. Manuel Blum and Dexter Kozen. On the power of the compass. In *Proc. 19th Annual Symposium on Found ations of Computer Sci*, pages 132–142, 1978.
15. Guido Bugmann, John G Taylor, and M Denham. Route finding by neural nets. *Neural networks*, pages 217–230, 1995.
16. Christopher I Connolly, JB Burns, and R Weiss. Path planning using Laplace's equation. In *Robotics and Automation, 1990. Proceedings., 1990 IEEE International Conference on*, pages 2102–2106. IEEE, 1990.
17. Alexander E Dubinov, Artem N Maksimov, Maxim S Mironenko, Nikolay A Pylayev, and Victor D Selemir. Glow discharge based device for solving mazes. *Physics of Plasmas (1994-present)*, 21(9):093503, 2014.
18. Michael J Fuerstman, Pascal Deschatelets, Ravi Kane, Alexander Schwartz, Paul JA Kenis, John M Deutch, and George M Whitesides. Solving mazes using microfluidic networks. *Langmuir*, 19(11):4714–4722, 2003.
19. Simon Goss, Serge Aron, Jean-Louis Deneubourg, and Jacques Marie Pasteels. Self-organized shortcuts in the Argentine ant. *Naturwissenschaften*, 76(12):579–581, 1989.
20. Simon Goss, R Beckers, Jean-Louis Deneubourg, Serge Aron, and Jacques M Pasteels. How trail laying and trail following can solve foraging problems for ant colonies. In *Behavioural Mechanisms of Food Selection*, pages 661–678. Springer, 1990.

21. Pavlos Gourtzelidis, Charidimos Tzagarakis, Scott M Lewis, David A Crowe, Edward Auerbach, Trenton A Jerde, Kâmil Uğurbil, and Apostolos P Georgopoulos. Mental maze solving: directional fMRI tuning and population coding in the superior parietal lobule. *Experimental brain research*, 165(3):273–282, 2005.
22. Tobias Haist and Wolfgang Osten. Wave-optical computing based on white-light interferometry. *DGaO Proceedings*, 2008.
23. Li-Da Huang and Martin DF Wong. Optical proximity correction: friendly maze routing. In *Proceedings of the 41st annual Design Automation Conference*, pages 186–191. ACM, 2004.
24. Yong K Hwang and Narendra Ahuja. A potential field approach to path planning. *Robotics and Automation, IEEE Transactions on*, 8(1):23–32, 1992.
25. SE Kemeny, TJ Shaw, RH Nixon, and ER Fossum. Parallel processor array for high speed path planning. In *Proc. 1992 IEEE Custom Integrated Circuits Conf., pp. P*, volume 6, pages 1–5, 1992.
26. Gul Muhammad Khan and Julian Francis Miller. Solving mazes using an artificial developmental neuron. In *ALIFE*, pages 241–248, 2010.
27. Oussama Khatib. Real-time obstacle avoidance for manipulators and mobile robots. *The international journal of robotics research*, 5(1):90–98, 1986.
28. Vladimir I Kolobov. Advances in electron kinetics and theory of gas discharges. *Physics of Plasmas (1994-present)*, 20(10):101610, 2013.
29. István Lagzi, Siowling Soh, Paul J Wesson, Kevin P Browne, and Bartosz A Grzybowski. Maze solving by chemotactic droplets. *Journal of the American Chemical Society*, 132(4):1198–1199, 2010.
30. Chin Yang Lee. An algorithm for path connections and its applications. *Electronic Computers, IRE Transactions on*, (3):346–365, 1961.
31. Petra Lovass, Michal Branicki, Rita Tóth, Artur Braun, Kohta Suzuno, Daishin Ueyama, and István Lagzi. Maze solving using temperature-induced Marangoni flow. *RSC Advances*, 5(60):48563–48568, 2015.
32. Vladimir J Lumelsky. A comparative study on the path length performance of maze-searching and robot motion planning algorithms. *Robotics and Automation, IEEE Transactions on*, 7(1):57–66, 1991.
33. Vladimir J Lumelsky and Alexander A Stepanov. Path-planning strategies for a point mobile automaton moving amidst unknown obstacles of arbitrary shape. *Algorithmica*, 2(1-4):403–430, 1987.
34. Aswathi Nair, Karthik Raghunandan, Vaddi Yaswant, Sreelal S Pillai, and Sanjiv Sambandan. Maze solving automatons for self-healing of open interconnects: Modular add-on for circuit boards. *Applied Physics Letters*, 106(12):123103, 2015.
35. Toshiyuki Nakagaki, Hiroyasu Yamada, and Agota Toth. Path finding by tube morphogenesis in an amoeboid organism. *Biophysical chemistry*, 92(1):47–52, 2001.
36. Ajay Narendra. Homing strategies of the Australian desert ant Melophorus bagoti I. Proportional path-integration takes the ant half-way home. *Journal of Experimental Biology*, 210(10):1798–1803, 2007.
37. Youichi Okabayashi, Takashi Isoshima, Etsushi Nameda, Song-Ju Kim, and Masahiko Hara. Two-dimensional nonlinear Fabry-Perot interferometer: An unconventional computing substrate for maze exploration and logic gate operation. *International Journal of Nanotechnology and Molecular Computation (IJNMC)*, 3(1):13–23, 2011.
38. VV Pavlov and AN Voronin. The method of potential functions for coding constraints of the external space in an intelligent mobile robot. *Soviet Automatic Control*, 17(6):45–51, 1984.
39. Yuriy V Pershin and Massimiliano Di Ventra. Solving mazes with memristors: A massively parallel approach. *Physical Review E*, 84(4):046703, 2011.
40. Véronique Pimienta and Charles Antoine. Self-propulsion on liquid surfaces. *Current Opinion in Colloid & Interface Science*, 19(4):290–299, 2014.
41. Jianhua Qin and Aaron R Wheeler. Maze exploration and learning in C. elegans. *Lab on a Chip*, 7(2):186–192, 2007.
42. NG Rambidi and D Yakovenchuk. Chemical reaction-diffusion implementation of finding the shortest paths in a labyrinth. *Physical Review E*, 63(2):026607, 2001.
43. Darwin R Reyes, Moustafa M Ghanem, George M Whitesides, and Andreas Manz. Glow discharge in microfluidic chips for visible analog computing. *Lab on a Chip*, 2(2):113–116, 2002.
44. Andy M Reynolds, Tushar K Dutta, Rosane HC Curtis, Stephen J Powers, Hari S Gaur, and Brian R Kerry. Chemotaxis can take plant-parasitic nematodes to the source of a chemo-attractant via the shortest possible routes. *Journal of the Royal Society Interface*, 8(57):568–577, 2011.
45. Vincent Ricigliano, Javed Chitaman, Jingjing Tong, Andrew Adamatzky, and Dianella G Howarth. Plant hairy root cultures as plasmodium modulators of the slime mold emergent computing substrate Physarum polycephalum. *Frontiers in microbiology*, 6, 2015.

46. Frank Rubin. The Lee path connection algorithm. *Computers, IEEE Transactions on*, 100(9):907–914, 1974.
47. Cally Scherber, Alexander J Aranyosi, Birte Kulemann, Sarah P Thayer, Mehmet Toner, Othon Iliopoulos, and Daniel Irimia. Epithelial cell guidance by self-generated EGF gradients. *Integrative Biology*, 4(3):259–269, 2012.
48. Claude E Shannon. Presentation of a maze-solving machine. In *8th Conf. of the Josiah Macy Jr. Found.(Cybernetics)*, pages 173–180, 1951.
49. Mircea R Stan, Wayne P Burleson, Christopher I Connolly, and Roderic A Grupen. Analog VLSI for robot path planning. *Analog Integrated Circuits and Signal Processing*, 6(1):61–73, 1994.
50. Oliver Steinbock, Ágota Tóth, and Kenneth Showalter. Navigating complex labyrinths: optimal paths from chemical waves. *SCIENCE-NEW YORK THEN WASHINGTON-*, pages 868–868, 1995.
51. Lois O Stratton and William P Coleman. Maze learning and orientation in the fire ant (Solenopsis saevissima). *Journal of comparative and physiological psychology*, 83(1):7, 1973.
52. L Tarassenko and A Blake. Analogue computation of collision-free paths. In *Robotics and Automation, 1991. Proceedings., 1991 IEEE International Conference on*, pages 540–545. IEEE, 1991.
53. Lionel Tarassenko, Michael Brownlow, Gillian Marshall, Jan Tombs, and Alan Murray. Real-time autonomous robot navigation using VLSI neural networks. In *Advances in neural information processing systems*, pages 422–428, 1991.
54. Atsushi Tero, Ryo Kobayashi, and Toshiyuki Nakagaki. Physarum solver: a biologically inspired method of road-network navigation. *Physica A: Statistical Mechanics and its Applications*, 363(1):115–119, 2006.
55. Charles Henry Turner. The homing of ants: An experimental study of ant behavior. *Journal of Comparative Neurology and Psychology*, 17(5):367–434, 1907.
56. Jitka Čejkova, Matej Novak, Frantisek Stepanek, and Martin M Hanczyc. Dynamics of chemotactic droplets in salt concentration gradients. *Langmuir*, 30(40):11937–11944, 2014.
57. Richard A Wallace. The maze solving computer. In *Proceedings of the 1952 ACM national meeting (Pittsburgh)*, pages 119–125. ACM, 1952.
58. David M Willardson. Analysis of micromouse maze solving algorithm. *Learning from Data*, 2001.
59. L Wyard-Scott and Q-HM Meng. A potential maze solving algorithm for a micromouse robot. In *Communications, Computers, and Signal Processing, 1995. Proceedings., IEEE Pacific Rim Conference on*, pages 614–618. IEEE, 1995.
60. Ken Yokawa, Neven Derrien-Maze, Stefano Mancuso, and FRANTIŠEK BALUŠKA. Binary decisions in maize root behavior: Y-maze system as tool for unconventional computation in plants. *International Journal of Unconventional Computing*, 10, 2014.
61. Hao Ming Zhang, Lian Soon Peh, and Ying Hai Wang. Study on flood-fill algorithm used in micromouse solving maze. In *Applied Mechanics and Materials*, volume 599, pages 1981–1984. Trans Tech Publ, 2014.
62. Shaowu Zhang, Akiko Mizutani, and Mandyam V Srinivasan. Maze navigation by honeybees: learning path regularity. *Learning & Memory*, 7(6):363–374, 2000.
63. Min Zhao and Andre G Marquez. Understanding humans' strategies in maze solving. *arXiv preprint arXiv:1307.5713*, 2013.